Earth's Future

RESEARCH ARTICLE
10.1029/2021EF002163

The Alaskan Summer 2019 Extreme Heat Event: The Role of Anthropogenic Forcing, and Projections of the Increasing Risk of Occurrence

Sarah K. Weidman[1,2], **Thomas L. Delworth**[2], **Sarah B. Kapnick**[2], **and William F. Cooke**[2]

[1]Department of Earth, Atmospheric and Planetary Sciences, Massachusetts Institute of Technology, Cambridge, MA, USA, [2]Geophysical Fluid Dynamics Laboratory, NOAA, Princeton, NJ, USA

Key Points:

- The presence of anthropogenic radiative forcing increased the likelihood of the 2019 extreme heat event by as much as 6%
- The rate of occurrence of such an extreme heat event is likely to substantially increase in the coming decades
- By the 2060s simulations suggest that such an extreme heat event could occur almost every other year, moving from a rare to a common event

Supporting Information:

Supporting Information may be found in the online version of this article.

Correspondence to:

S. K. Weidman,
sweidman@g.harvard.edu

Citation:

Weidman, S. K., Delworth, T. L., Kapnick, S. B., & Cooke, W. F. (2021). The Alaskan summer 2019 extreme heat event: The role of anthropogenic forcing, and projections of the increasing risk of occurrence. *Earth's Future*, *9*, e2021EF002163. https://doi.org/10.1029/2021EF002163

Received 30 APR 2021
Accepted 29 JUL 2021

Author Contributions:

Conceptualization: Sarah K. Weidman, Thomas L. Delworth, Sarah B. Kapnick
Data curation: William F. Cooke
Formal analysis: Sarah K. Weidman
Investigation: Sarah K. Weidman

Abstract Extreme heat occurred over Alaska in June–July 2019, posing risks to infrastructure, ecosystem, and human health. It is vital to improve our understanding of the causes of such events and the extent to which anthropogenic forcing may alter their likelihood and magnitude. Here, we use multiple large ensembles of climate models, comprising thousands of simulated years, to investigate these issues. Our results suggest that the presence of anthropogenic radiative forcing increased the likelihood of the 2019 extreme heat event by as much as 6%. Further we show the rate of occurrence of such an extreme heat event is likely to substantially increase in the future with increasing levels of atmospheric greenhouse gases. While uncertainty in projected climate risk from model choice leads to a broad range of future extreme heat event probabilities, some models project that with rapidly increasing levels of greenhouse gases the likelihood of such events would exceed 75% by 2090.

Plain Language Summary An extended period of high temperatures across the state of Alaska in June and July, 2019 set multiple temperature records. Here, we examine the extent to which human-driven climate change played a role in increasing the likelihood of experiencing such an extreme event. Using global climate models, we determine that human-driven climate change increased the probability of experiencing such high temperatures in 2019, and that the likelihood of similar or more extreme events will increase into the coming century.

1. Introduction

1.1. Background

In June and July, 2019, Alaska experienced an extended period of record high temperatures. Temperatures at several weather stations broke all-time records; in Anchorage, temperatures reached 32°C, breaking records by 3°C (Di Liberto, 2019). Temperatures remained abnormally high from approximately June 23–July 10, with Anchorage breaking 27°C for six consecutive days (another record).

In Alaska, increasing temperatures have significant societal and economic effects: degrading permafrost can result in damages to roads and infrastructure as soils sink (Melvin et al., 2017), shifting marine ecosystems can cause serious damage to Alaska's vitally important fish and crab industry (Thorsteinson & Love, 2016), and increasing wildfire risk can pose risk to many communities (Young et al., 2017, Yu et al., 2021). The risk of highly active and damaging fire seasons such as in the summer of 2015 has been shown to have increased by 35%–60% due to anthropogenic forcing (Partain et al., 2016). Damages in Alaska due to human-induced climate change are expected to range from $110 to $270 million per year and will disproportionately affect Alaska's rural and Indigenous communities (Cochran et al., 2013; Gray et al., 2018). The extent of future warming and expected frequency of extreme heat events in the region are still uncertain, and thus it is vital to increase our understanding of observed events and improve our ability to quantify present and future climate risk.

Extreme heat events have frequently been observed in Arctic regions in the last decade (Thoman & Brettschneider, 2016), likely the result of anthropogenic climate change. Observations can be used to quantify changes in temperature over the past several decades, while climate models can be used to project future warming—which may accelerate—and changes in frequency of extreme heat events. Studies analyzing observed climate identify clear warning signals over the Arctic at a faster rate than much of the planet; this polar

Methodology: Sarah K. Weidman, Thomas L. Delworth, Sarah B. Kapnick
Software: Sarah K. Weidman, William F. Cooke
Supervision: Thomas L. Delworth, Sarah B. Kapnick
Visualization: Sarah K. Weidman
Writing – original draft: Sarah K. Weidman
Writing – review & editing: Thomas L. Delworth, Sarah B. Kapnick, William F. Cooke

amplification results in an observed trend in warming twice as strong over the Arctic from 1875 to 2008 than over the Northern Hemisphere as a whole (Bekryaev et al., 2010), and this rate has continued through 2019 (Overland et al., 2020). However, there is high natural variability in the Arctic, due to multi-decadal variability in changing sea surface temperature and sea ice trends (Chylek et al., 2009; Steele et al., 2008). Large ensemble climate models can simulate the changes in temperature and frequency of extreme heat events at a local (state-wide) scale (Lader et al., 2017), quantifying the probability of an event over time. A large ensemble can provide sufficient data to detect changes in risk from anthropogenic climate change, especially critical in regions with large internal variability like the Arctic.

The high natural variability, recent accelerated trends in warming, and major economic impacts over the Arctic make quantifying changes in extreme heat events, and their uncertainty, of high importance. Studies have pursued similar questions for several extreme heat events in the Arctic, such as the 2020 extreme heat in Siberia (Overland & Wang, 2021), the 2016 Alaskan marine heat wave (Walsh et al., 2018), the highly active 2015 Interior Alaska fire season (Partain et al., 2016), and the trend of warming over the Arctic (Chylek et al., 2014). In each of these studies, extreme heat and warming can be at least partially attributed to anthropogenic emissions, but a study of this sort has not yet focused on the extreme heat event over Alaska in June–July 2019. Beyond attributing this event to climate change, estimating the future likelihood of similar extreme heat events will be critical for informing policies and infrastructure to build future resiliency. In this study, we assess whether the high temperatures recorded in June and July 2019 over Alaska can be attributed to anthropogenic forcings. We then quantify the likelihood of observing a similar extreme heat event in the coming century, using large ensembles of projections of future climate change from multiple climate models.

1.2. June–July 2019 Extreme Heat Event Over Alaska

Most of the state of Alaska experienced anomalously high temperatures for an extended duration in early summer 2019, extending from approximately June 23–July 10 (Voiland et al., 2019). Figure 1a displays the region with the strongest anomalous temperatures during this event, where temperatures exceeded the mean temperature by more than 1.5°C relative to the 1980–2010 period. Observed June–July raw air temperatures from 2019 compared to previous years are displayed in Figure 1b. We will refer to this event as the 2019 extreme heat event. Normalized observed temperatures are shown in Figure 1c, where air temperatures are normalized by the 1921–1960 June–July interannual standard deviation, described in more detail in the following section. High temperatures in June–July 2019 were associated with a large dome of high pressure over southeast Alaska, allowing for high surface temperatures to linger (Di Liberto, 2019).

Coincident with the anomalously high air temperatures over Alaska, the North Pacific saw anomalously high summer sea surface temperatures and record low summer sea ice extent (Alaska Climate Review, 2019). Following the record high temperatures in early summer, an extremely active fire season continued through August 2019, burning over 2.5 million acres, double the mean number of acres burned each season from 2010 to 2019 (Strader & Stevens, 2019; Yu et al., 2021). In particular, some of this late-season extreme fire activity occurred over Southcentral Alaska, which is unusual for that region (Bhatt et al., 2021). June-July, 2004 also recorded high temperatures of a similar magnitude (Figure 1b), again coincident with extensive burning during an exceptionally active forest fire season (Duck et al., 2007).

2. Methods

Analyses of projected temperature extremes were performed using large ensembles of simulations from a recently developed coupled climate model called "SPEAR" (Seamless System for Prediction and EArth System Research) (Delworth et al., 2020). This model is designed as a seamless prediction and projection system that focuses on time scales from seasonal to multidecadal, and is used for real-time seasonal prediction (Kirtman et al., 2014), real-time decadal prediction (see https://hadleyserver.metoffice.gov.uk/wmolc/), and multidecadal climate projection. The model horizontal resolution is approximately 50 km for the atmosphere and land components, comparable to regional climate model ensembles such as CORDEX (Mearns et al., 2017). The horizontal resolution is approximately 1° over ocean and sea ice. We used monthly mean surface air temperature output from three separate 30-member ensembles. The first ensemble extends

10.1029/2021EF002163

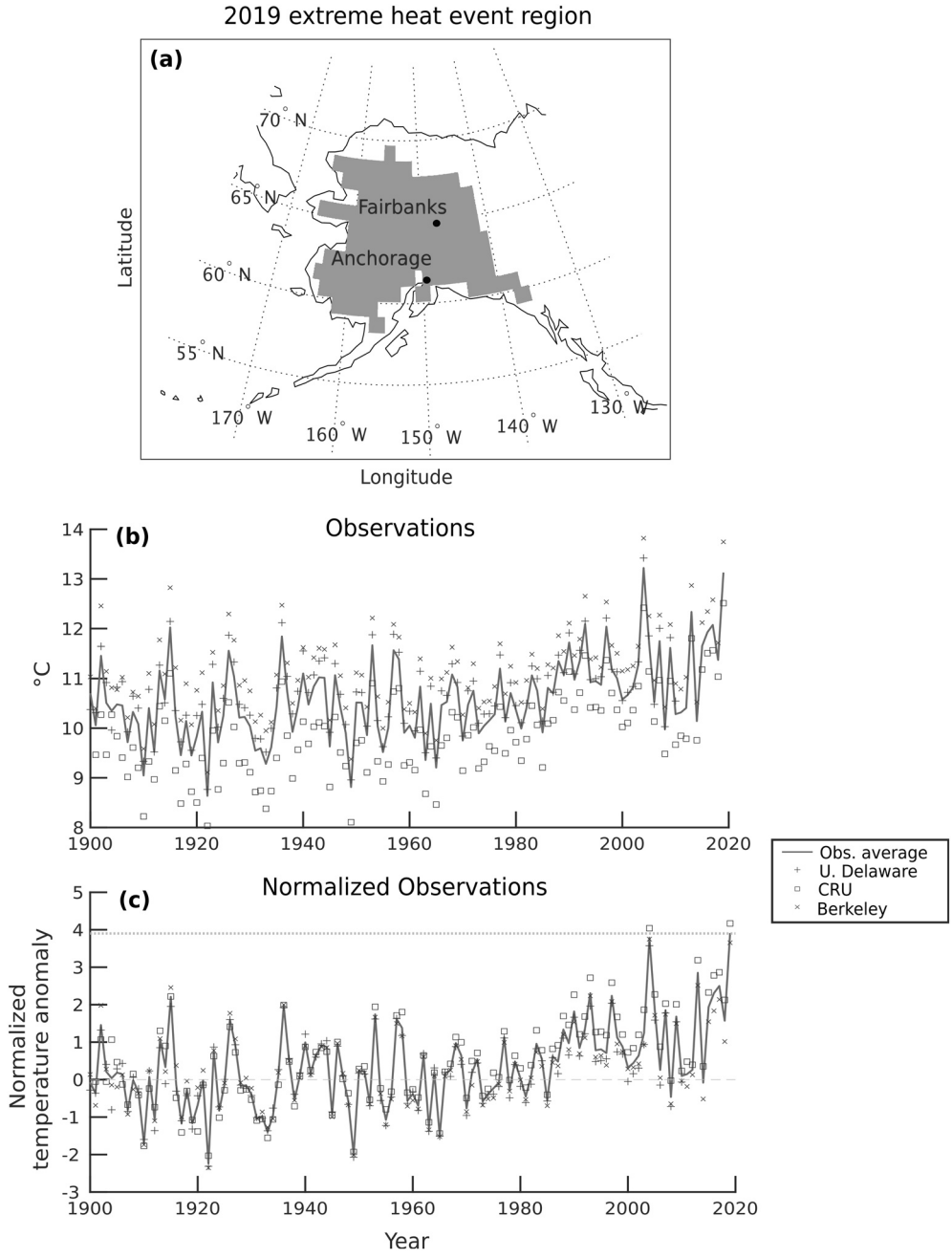

Figure 1. Observed June–July temperatures over Alaska. The shaded region in (a) shows the gridpoints in which June–July 2019 mean temperatures were greater than 1.5°C higher than the 1981–2010 mean. (b) Displays a time series of the observed June–July mean 2-m temperatures averaged over the region in (a). (c) is the same as (b) but with normalized temperature anomalies, using 1921–1960 as a climatology period and normalizing by the 1921–1960 June–July interannual standard deviation. The solid line represents the average June–July temperature of the observational data sets. The dotted line in (c) marks the 2019 normalized June–July temperature.

from 1921 to 2100, and uses historical radiative forcing over the period 1921–2014, and projected radiative forcings using the Shared Socioeconomic Pathways 5–8.5 scenario (abbreviated as SSP5-8.5) for the period 2015–2100 (O'Neill et al., 2016). During the historical period this forcing consists of observationally based estimates of changes in greenhouse gases, anthropogenic and natural aerosols, and solar irradiance changes. The 30 members of the ensemble were initialized from a long preindustrial control simulation, with starting points taken every 20 years. This ensemble is called "HIST_SSP585." A second 30-member ensemble was

Table 1
Detailed Model Information

Data set	Institute	Horizontal resolution	Simulations	Number of ensemble members	Transient climate response (K)	Reference
SPEAR-MED	GFDL	0.5° land and atmosphere; 1° ocean and sea ice	NATURAL; HIST_SSP245; HIST_SSP585	30	1.78	(Delworth et al., 2020)
CESM1	NCAR	1° atmosphere, ocean, land, sea ice	RCP 8.5	40	2.3	(Kay et al., 2015)(Hurrell et al., 2013)
MPI-GE	Max Planck Institute for Meteorology	1.8° atmosphere; 1.5° ocean	RCP 4.5; RCP 8.5	100	2.0	(Maher et al., 2019) (Giorgetta et al., 2013)

run for 1921–2100 using only radiative forcing changes from natural sources (volcanic aerosols and solar irradiance changes), but anthropogenic forcing kept fixed at calendar year 1921. This ensemble is called "NATURAL." A third ensemble was run for the period 2015–2100 using radiative forcings from the SSP2-4.5 scenario. We combine the output from the ensemble using historical forcing over 1921–2014 with the output from the ensemble using SSP2-4.5 forcing over the period 2015–2100 to form the "HIST_SSP245" ensemble. Later in the paper we also use ensembles from two additional coarser-resolution models using relative concentration pathways (RCPs). Detailed information about the models is listed in Table 1.

To assess the ability of the models to simulate observed temperature over Alaska, we used three gridded observational data sets: Berkeley Earth (Rohde, Muller, Jacobsen, Muller, et al., 2013; Rohde, Muller, Jacobsen, Perlmutter, et al., 2013), University of Delaware (Willmott & Matsuura, 2001), and CRU TS4.04 (Harris et al., 2020; Morice et al., 2012). These data sets were selected because they reported gridded temperature data for Alaska through at least 1921–1960, the climatology period used to assess the model's simulation of temperature seasonal cycles. Both the Berkeley Earth and CRU data sets reported observed temperatures through July 2019 and were used to characterize the 2019 extreme heat event. Given the persistence of the 2019 extreme heat event over several weeks in June and July, we choose to analyze June-July mean 2 m air temperature instead of over a few days to quantify the probability of this event both in the current climate and in future climates. Our region of interest is defined in Figure 1a where observed June–July mean temperatures in 2019 showed a positive anomaly of at least 1.5°C compared to the mean temperature from 1981 to 2010 (the same period as the Climate Normals used by the National Weather Service) in both the Berkeley Earth and CRU observations. Unless otherwise specified, regional averages are taken over the shaded region in Figure 1a.

We compared the seasonal cycle of model simulated temperature to the observed seasonal cycle over the period 1921–1960. We used this period for our climatology because we observe no clear warming or cooling trend during this 40-year period in the observations nor in the historical simulation of the model, so most interannual variability is likely due to internal variability of the climate system, rather than radiatively forced warming. Over 1921–1960, SPEAR displayed, on average, a 2–3 K cold bias over the full year. Similarly, we compared the 1921–1960 interannual standard deviation of June–July mean temperature to the standard deviation of observed June-July temperature. Each of the model's ensemble members has a slightly different standard deviation; thus, the minimum and maximum standard deviations out of all 30 ensemble members form a range of simulated standard deviations at each gridpoint. We determine that the model is able to simulate observed interannual variability if the observed 1921–1960 interannual standard deviation at that gridpoint falls within this range. By this metric, 69% of the model grid points in our region of interest simulate interannual variability consistent with observations. The exception is in the northern third of the state, as well as regions near the southern coastline (Figure S1a).

To account for biases in the model's representation of observed Alaskan temperatures and their interannual variability, we first calculate normalized temperature anomalies by subtracting the 1921–1960 time-mean temperature and dividing by the standard deviation. This was done for both observational and model data sets, using their respective means and standard deviations. This normalization is represented as:

$$T_{normalized} = \frac{(T - \bar{T}_{clim})}{\sigma_{clim}}. \quad (1)$$

Figure 1c shows the observed normalized temperatures from 1900 to 2019. Only the Berkeley Earth and CRU data sets have released temperature observations through July 2019 at the time of writing. The average normalized temperature for the 2019 extreme heat event for these two data sets was 3.9; we choose this value as our lower bound threshold for classifying extreme heat events in the models.

After the initial analysis with SPEAR, we analyzed large ensembles from two additional models to assess the sensitivity of our results to model formulation. We used output from the Max Planck Institute Grand Ensemble (MPI-GE) (Maher et al., 2019), and the Community Earth System Model version 1 (CESM1) (Kay et al., 2015). These models employed radiative forcing scenarios developed for CMIP5: RCP 4.5 and RCP 8.5 for MPI-GE and RCP 8.5 for CESM1 (Table 1). Following the same procedure as described above, we assessed the ability of CESM1 and MPI-GE to simulate observed Alaskan temperatures. CESM1 displayed a 1–2 K warm bias over June–August and a 4 K cold bias in winter months. MPI-GE showed little bias in June and November temperatures, but otherwise displayed a 3–4 K cold bias during the rest of the year. An average of 41% and 27% of grid points in our region of interest were able to capture the interannual variability of the observations for MPI-GE and CESM1, respectively (Figure S1). Standard deviations in these two models exceeded the observed standard deviation by on average 0.45 and 0.58 respectively, compared to an average observed standard deviation of 0.76.

3. Results

3.1. Role of Anthropogenic Forcing in the 2019 Extreme Heat Event

To determine whether anthropogenic forcing increased the likelihood of an extreme heat event such as in June–July 2019 in Alaska, we compare the likelihood of simulating similar extreme heat events in the ensembles using SSP or RCP scenarios to the ensemble using NATURAL forcings. If anthropogenic forcing played a significant role in increasing that likelihood, we would expect the SSP or RCP forced ensembles to simulate 2019-like events at a significantly higher rate than in the NATURAL forcing scenario. Events are considered to be as extreme or more extreme than the 2019 extreme heat event if the normalized temperature exceeds the 3.9 threshold as calculated for the observed 2019 extreme heat event.

We compare the frequency of simulating normalized temperatures surpassing the 3.9 threshold during current decades (2011–2030) in the anthropogenic forcing scenarios to the natural forcing scenario. Normalized June–July temperatures from 1921 to 2100 as simulated by each forcing scenario are plotted in Figure 2. Shading represents the minimum and maximum normalized temperatures simulated by any of the ensemble members within that forcing scenario. Any shading that exceeds the dotted line represents one or more ensemble members surpassing the 3.9 threshold. The likelihood that various ensembles simulate an event above the 3.9 threshold in a given decade is listed in Table 2. Results from the NATURAL ensemble are not shown in Table 2 since this ensemble generates no cases with temperature above the threshold. Probabilities above 50% are in bold to show the decades at which surpassing the extreme heat event threshold become a "median" event.

There is a greater likelihood of surpassing the 3.9 threshold in the anthropogenic forcing scenarios during current decades than in the NATURAL ensemble. In the NATURAL ensemble (Figure 2a), there are no years in which normalized temperatures in any ensemble member surpass the 3.9 threshold. Conversely, in every anthropogenic forcing scenario, at least one ensemble member simulated normalized temperatures above the 3.9 threshold in 2011–2030. The likelihood of experiencing temperatures as high as the 2019 extreme heat event in the anthropogenic forcing scenarios range between 0.35% and 6% from 2011 to 2030, compared to 0% in the NATURAL ensemble. Since we only see temperatures above the 3.9 threshold in simulations with anthropogenic forcing, these model results suggest that human-induced radiative forcing made the 2019 extreme heat event more likely than otherwise.

10.1029/2021EF002163

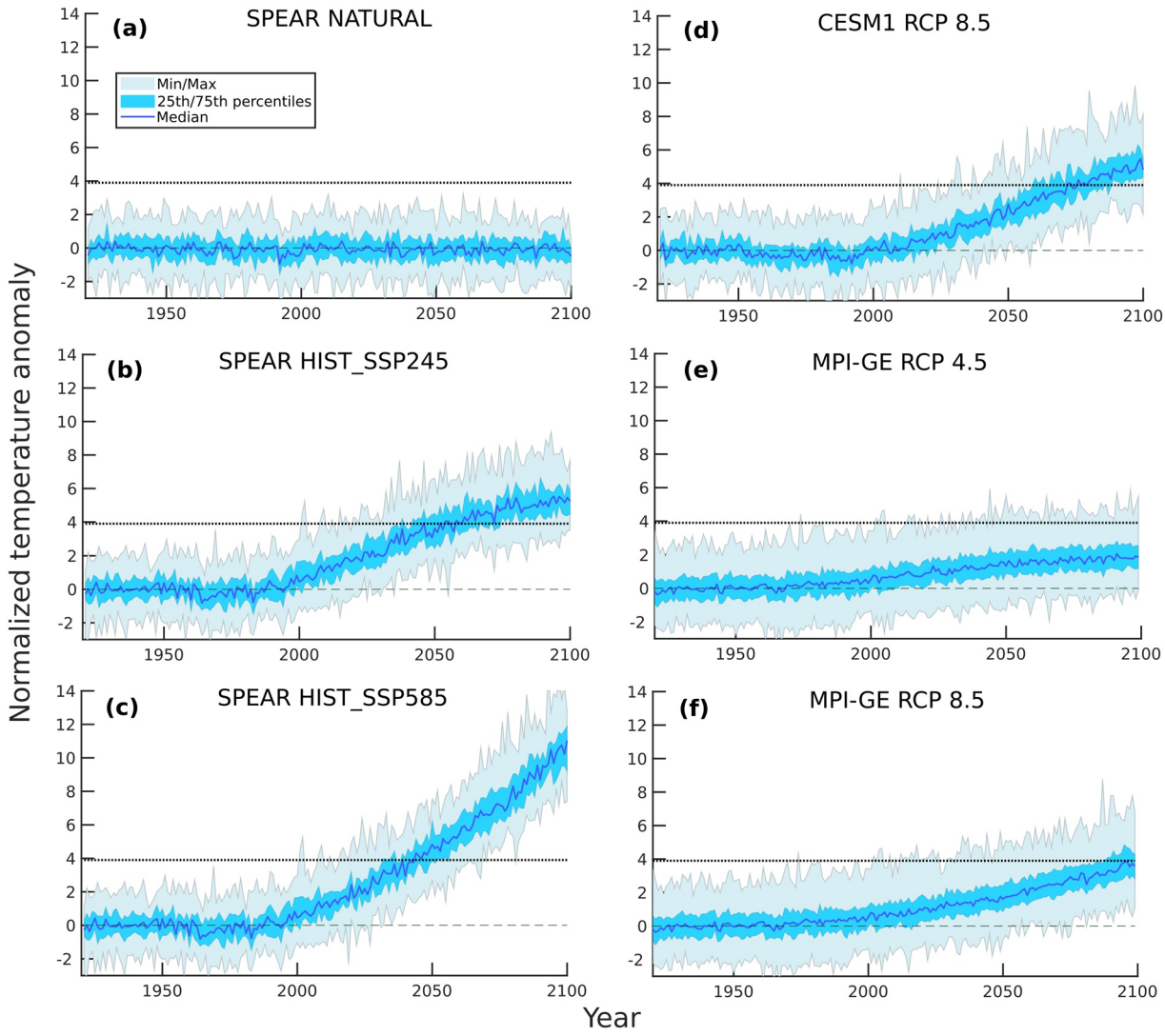

Figure 2. June-July normalized temperatures (dimensionless, see Equation 1) in model simulations from 1921 to 2100. (a–c) are the three forcing pathways from SPEAR: the NATURAL ensemble, HIST_SSP245, and HIST_SSP585, respectively. (d) is the CESM1 RCP 8.5 and (e and f) are the MPI-GE RCP 4.5 and RCP 8.5. The dark blue line is the median temperature out of all ensemble members, the inner blue shading marks the 25th and 75th percentiles, and the light blue shading marks the minimum and maximum. The dotted black line is the 3.9 threshold. Any shading above the threshold line represents an extreme heat event simulated in one or more of the ensemble members.

3.2. Likelihood of Extreme Heat in the Future

Using the simulated anthropogenic forcing scenarios, we can quantify the likelihood over time of temperatures exceeding the June-July 2019 threshold over Alaska. Figures 2b–2f and Table 2 describe these changes over the period from 1921 to 2100. Normalized temperatures do not exceed the 3.9 threshold in any scenario before 2000, so decades before 2001–2010 are not listed in Table 2. At the beginning of the 21st century, temperatures surpassing the 3.9 threshold are unlikely; only one or two ensemble members simulate June–July temperatures above the 3.9 standard deviation threshold. However, the likelihood of surpassing the 3.9 threshold increases throughout the century in all forcing scenarios. The HIST_SSP585 ensemble with SPEAR projects the most vigorous increase in the likelihood of extreme heat events through the 21st century, simulating June–July temperatures above the 3.9 threshold in nearly every ensemble member after 2071. Differences between each scenario will be discussed in the next section.

We also examine changes over time in the distribution of June-July temperatures simulated in the SPEAR HIST_SSP585 and HIST_SSP245 ensembles, and compare changes in the likelihood of extreme events to

Table 2
Probabilities of Surpassing the 3.9 Extreme Heat Event Threshold[a]

	SPEAR		CESM1	MPI-GE	MPI-GE
Decade	HIST_SSP245	HIST_SSP585	RCP 8.5	RCP 4.5	RCP 8.5
2001–2010	1.3%	1.3%	0.3%	0.3%	0.4%
2011–2020	2.7%	3.0%	0.0%	0.4%	1.1%
2021–2030	5.3%	9.0%	1.0%	0.4%	1.0%
2031–2040	18.3%	28.0%	2.3%	0.7%	2.2%
2041–2050	33.3%	**57.3%**	7.8%	1.9%	2.2%
2051–2060	47.3%	**78.7%**	15.5%	2.5%	5.2%
2061–2070	**67.7%**	**95.3%**	32.5%	1.9%	10.2%
2071–2080	**76.3%**	**100.0%**	49.8%	2.9%	15.2%
2081–2090	**80.7%**	**99.7%**	**69.0%**	4.4%	23.0%
2091–2100	**87.3%**	**100.0%**	**81.3%**	4.1%	39.4%

Note. Probabilities above 50% in bold.

[a]Percent of times an ensemble records a temperature above the 3.9 threshold with a sample size = number of ensemble members multiplied by 10 years.

decadal distributions of the NATURAL ensemble. In 1991–2000, the simulated temperature distributions approximately match the shape and spread of the control climate. In later decades, the center of the distributions from the SSP runs moves to the right, while the standard deviation of the distributions increase slightly from 1.1 to about 1.3. From 2001 to 2020, events that surpass the 3.9 threshold are at the extreme maximum of the temperature distribution. However, in later decades, a greater proportion of the distribution surpasses the threshold simply due to a shift in the center of the distribution. Figure 3 suggests that the higher probabilities of extreme heat events in later decades is not due to an increasing frequency of *extreme* events (events at the extreme ends of a distribution), but rather an increase in the entire distribution of temperatures. For example, June–July simulated temperatures that in 2020 would be considered extreme would be near the median of the distribution in 2050.

3.3. Sensitivity of Results

The likelihoods of simulating temperatures above the 3.9 threshold differ between forcing scenario and model. Probabilities do not differ much between the HIST_SSP245 and HIST_SSP585 pathways for the next several decades. However, the two pathways begin to diverge by 2041–2050 with the HIST_SSP585 increasing much more quickly than the HIST_SSP245. Both CESM1 and MPI-GE also project increased likelihoods of June–July temperatures above the 3.9 threshold, though the rate and magnitude of increase differ. Both models project a smaller overall increase in normalized temperatures by the end of the century than the HIST_SSP585 simulation. The discrepancy between models is partially due to the normalization process. As described in Section 2, the standard deviations of June-July temperature in every ensemble member for both MPI-GE and CESM1 are higher than in SPEAR and the observed values in most Alaskan regions. Since we use standard deviation as our normalization factor, it follows that the normalized increase in temperature would be muted for MPI-GE and CESM1 due to their higher standard deviation. Raw values for median increase in June-July temperatures by 2100 are comparable between the HIST_SSP585 and CESM1 RCP 8.5 run: about 8–9 K. HIST_SSP245 and MPI-GE RCP 8.5 increase by about 4–5 K by 2100, and MPI-GE RCP 4.5 increases by 2 K. Further differences between the models are likely due to differences in model construction: a display of model uncertainty.

We tested how sensitive our results are to the initial choice of a threshold temperature to define the region of extreme heat in the 2019 event. We found that varying this criterion modified some details of the quantitative aspects of the findings, but the central conclusions are robust to that choice. Adjusting the region of interest in Figure 1a to be any land region where June–July 2019 temperatures were greater than 1°or 2°C above the 1980–2010 mean temperature in the observations changes the likelihood of experiencing the 2019 extreme heat event to 6% and 3%, respectively, using the HIST_SSP585 scenario.

4. Discussion

We have demonstrated that the extreme heat during June–July 2019 in Alaska is at least partially attributable to anthropogenic climate change. For 2011–2030, models project that the 2019 extreme heat event would be a low probability event, but still within the realm of possibility. Without anthropogenic forcing the models suggest this type of event would not be possible. However, with anthropogenic forcing the entire temperature distribution shifts to warmer values over time. By 2100, the 2019 extreme heat event in the SPEAR model becomes an average event under HIST_SSP245 and part of the colder tail of the distribution under HIST_SSP585. An event that was once an extreme heat event becomes a regular occurrence under both scenarios (Table 2, Figure 3). These results hold across models and forcing scenarios, despite differences in model transient climate response and strength of the anthropogenic forcing.

10.1029/2021EF002163

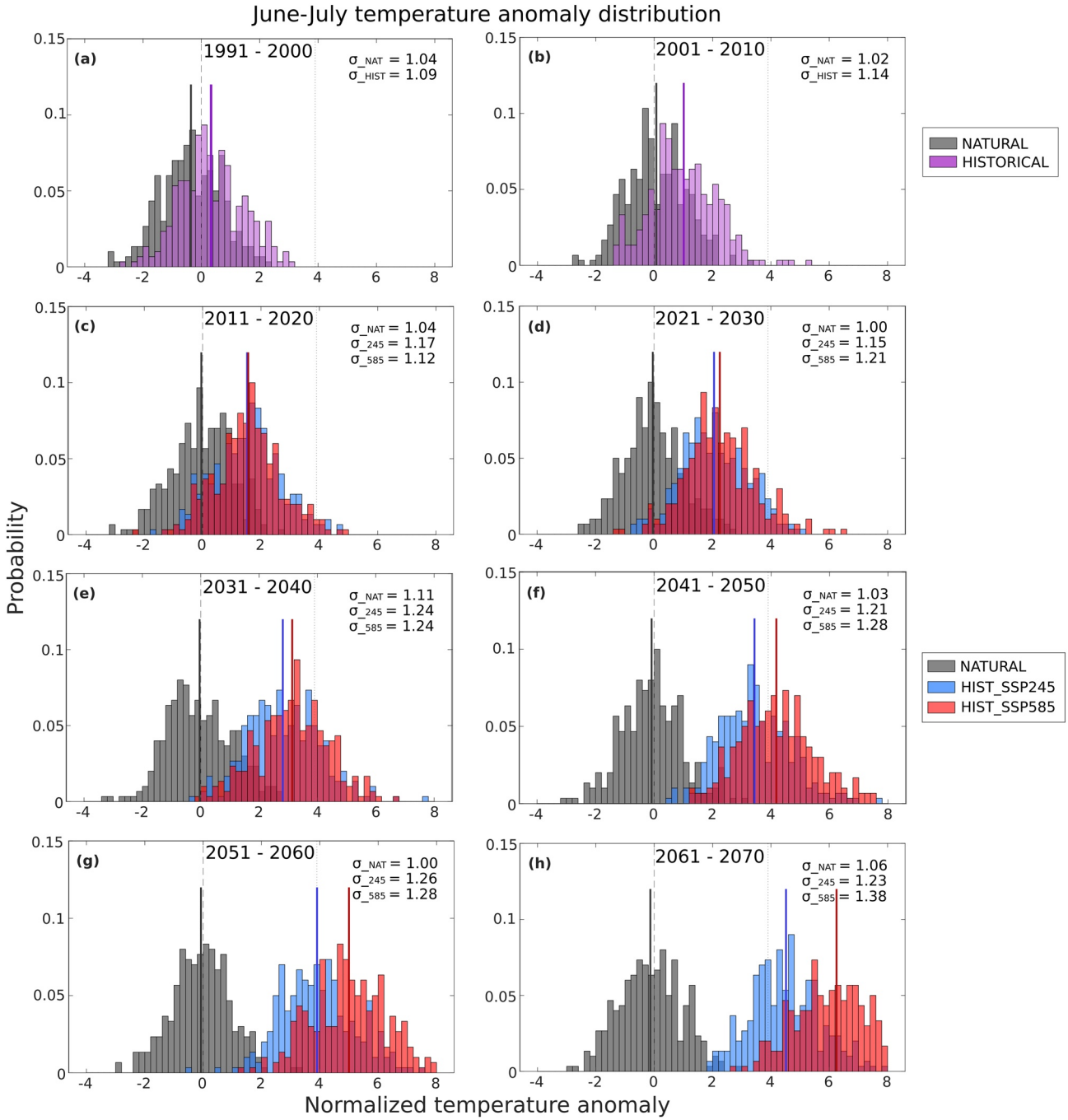

Figure 3. Decadal distributions of normalized temperatures (dimensionless, see Equation 1) for the NATURAL (gray), historical (purple), HIST_SSP245 (blue) and HIST_SSP585 (red) forcing pathways. Distributions in (c) consist of both the historical (2011–2014) and SSP ensembles (2015–2020). The distributions show the frequency of simulating a June–July normalized temperature by any of the ensemble members during each decade. Values to the right of the black dotted line exceed the observed 3.9 threshold; this occurs more frequently in later decades as the temperature distributions shift upwards. Mean values of each distribution are marked by solid vertical lines, with standard deviations listed in the corner.

Each scenario in Figure 2 projects an increase in likelihood of seeing events at least as strong as the 2019 extreme heat event; the uncertainty in the results instead comes from the rate of increase in temperature as projected by different GCMs and by different anthropogenic forcing pathways. Over the next 10–20 years, differences in likelihoods of seeing extreme heat events between different forcing pathways (Table 2) are fairly small, and most uncertainty in our results comes from differences between models. Starting in about

the 2040s the climate pathways start to diverge significantly. This follows from previous understanding of climate uncertainty; the importance of model uncertainty dominates in the near term, and only in a multi-decadal time scale does pathway uncertainty play a similarly dominant role (Hawkins & Sutton, 2011; Monier & Gao, 2014).

Models differ in many ways that could lead to the differences we see in their simulation of extreme heat over Alaska. These factors contribute to the uncertainty in projections, and include the following:

1. Each model simulates differing responses to increases in greenhouse gas concentrations as indicated by their differing transient climate responses, but what the response should be is not tightly constrained (Sherwood et al., 2020). Table 1 displays the differences in transient climate response between the three GCMs, which could affect differences in Alaskan temperatures by 2100.
2. SPEAR has a higher resolution than both other global models. Future work is necessary to determine how differences in model resolution affect the simulation of regional climate changes.
3. Each model differs in how they simulate sea ice, high latitude dynamics, and coupling with the land surface, all of which are significant in Arctic climate change (Castro-Morales et al., 2014; Loranty et al., 2014). These differences are more difficult to elucidate and are an active topic of research.

In the short term, most of the spread in changes in risk arise from differences in models, while at the end of the century, this spread depends on choice of forcing pathway. Because of the uncertainties between models, using multiple models in analyses can give a more comprehensive estimate of future climate change.

The 2019 extreme heat event occurred at the same time as a marine heat wave in the North Pacific. Although the causal relationship between these two events is unclear, future studies could attempt to evaluate whether extreme heat events over Alaska are typically associated with warm sea surface temperature anomalies. A relationship between these events could help with seasonal climate predictions—our results say nothing about whether an extreme heat event will occur in a certain year, rather that the probability of the event is increasing with time.

Further work could use the ranges of simulated temperatures between models to investigate the future climate implications of these rising temperatures. Tighter estimates of temperature extremes could help predict rates of sea ice loss, fire frequency, and changes in ecosystems (Gray et al., 2018). Risk of wildfire activity depends on both changes in temperature and precipitation, so analysis of temperature extremes could enhance attribution studies of active fire seasons to human-driven climate change, including the highly active fire season in August 2019 (Bhatt et al., 2021). Higher temperatures can also have harmful effects on human health, especially without adequate preparation as air conditioners and public cooling centers are not widely available in Alaska. Given the impacts and potential for prediction associated with other large scale features, further understanding of extreme heat events could advance seasonal prediction for advanced planning to reduce negative impacts on lives and property.

Data Availability Statement

SPEAR provided by the Geophysical Fluid Dynamics Laboratory with data available on the GFDL data portal and described on the SPEAR website: https://www.gfdl.noaa.gov/spear/. CESM1 provided by the CESM Large Ensemble Community Project from their website, https://www.cesm.ucar.edu/, and supercomputing resources provided by NSF/CISL/Yellowstone. MPI-GE provided by the Max Planck Institute for Meteorology at their website https://mpimet.mpg.de. UDel_AirT_Precip data provided by the NOAA/OAR/ESRL PSL, Boulder, Colorado, USA, from their website at https://psl.noaa.gov/. Berkeley Earth observations were downloaded from their website http://berkeleyearth.org/data/. HadCRUT4.6.0.0 data provided by Climatic Research Unit (University of East Anglia) and Met Office on their website https://crudata.uea.ac.uk/cru/data/temperature/.

Acknowledgments
This project was funded by the NOAA Ernest F. Hollings Undergraduate Scholarship Program. Additional financial support for this work was provided through base funding from the National Oceanic and Atmospheric Administration to the Geophysical Fluid Dynamics Laboratory. Conversations with Brian Brettschneider and Renee Tatusko were valuable in shaping the research questions addressed. The authors thank Liwei Jia and Yan Yu for their helpful comments and suggestions on the manuscript, and to two anonymous reviewers for their thoughtful feedback.

References

Alaska Climate Review. (2019). Retrieved from http://climate.gi.alaska.edu/sites/Default/Files/2019_AnnualReport.pdf

Bekryaev, R. V., Polyakov, I. V., & Alexeev, V. A. (2010). Role of polar amplification in long-term surface air temperature variations and modern Arctic warming. *Journal of Climate*, *23*(14), 3888–3906. https://doi.org/10.1175/2010jcli3297.1

Bhatt, U. S., Lader, R. T., Walsh, J. E., Bieniek, P. A., Thoman, R., Berman, M., & Ziel, R. (2021). Emerging anthropogenic influences on the Southcentral Alaska temperature and precipitation extremes and related fires in 2019. *Land*, *10*(1), 82. Retrieved from https://www.mdpi.com/2073?445X/10/1/82

Castro-Morales, K., Kauker, F., Losch, M., Hendricks, S., Riemann-Campe, K., & Gerdes, R. (2014). Sensitivity of simulated Arctic sea ice to realistic ice thickness distributions and snow parameterizations. *Journal of Geophysical Research: Oceans*, *119*(1), 559–571. https://doi.org/10.1002/2013JC009342

Chylek, P., Folland, C. K., Lesins, G., Dubey, M. K., & Wang, M. (2009). Arctic air temperature change amplification and the Atlantic Multidecadal Oscillation. *Geophysical Research Letters*, *36*(14), L14801. https://doi.org/10.1029/2009GL038777

Chylek, P., Hengartner, N., Lesins, G., Klett, J. D., Humlum, O., Wyatt, M., & Dubey, M. K. (2014). Isolating the anthropogenic component of Arctic warming. *Geophysical Research Letters*, *41*(10), 3569–3576. https://doi.org/10.1002/2014GL060184

Cochran, P., Huntington, O. H., Pungowiyi, C., Tom, S., Chapin, F. S., Huntington, H. P., et al. (2013). Indigenous frameworks for observing and responding to climate change in Alaska. *Climatic Change*, *120*, 557–567. https://doi.org/10.1007/s10584-013-0735-2

Delworth, T. L., Cooke, W. F., Adcroft, A., Bushuk, M., Chen, J.-H., Dunne, K. A., et al. (2020). SPEAR: The next generation GFDL modeling system for seasonal to multidecadal prediction and projection. *Journal of Advances in Modeling Earth Systems*, *12*(3), e2019MS001895. https://doi.org/10.1029/2019MS001895

Di Liberto, T. (2019). *High temperatures smash all-time records in Alaska in early July 2019*. Retrieved from https://www.climate.gov/news-features/event-tracker/high-temperatures-smash-all-time-records-alaska-early-july-2019

Duck, T. J., Firanski, B. J., Millet, D. B., Goldstein, A. H., Allan, J., Holzinger, R., & van Donkelaar, A. (2007). Transport of forest fire emissions from Alaska and the Yukon Territory to Nova Scotia during summer 2004. *Journal of Geophysical Research*, *112*(D10), D10S44. https://doi.org/10.1029/2006JD007716

Giorgetta, M. A., Jungclaus, J., Reick, C. H., Legutke, S., Bader, J., Böttinger, M., et al. (2013). Climate and carbon cycle changes from 1850 to 2100 in MPI-ESM simulations for the Coupled Model Intercomparison Project phase 5. *Journal of Advances in Modeling Earth Systems*, *5*(3), 572–597. https://doi.org/10.1002/jame.20038

Gray, S., Berman, M., Eerkes-Medrano, L., Hennessy, T., Huntington, H., Littell, J., et al. (2018). Alaska. In *Impacts, risks, and adaptation in the United States: Fourth National Climate Assessment* (Vol. II). https://doi.org/10.7930/NCA4.2018.CH26

Harris, I., Osborn, T. J., Jones, P., & Lister, D. (2020). Version 4 of the CRU TS monthly high-resolution gridded multivariate climate dataset. *Scientific Data*, *7*. https://doi.org/10.1038/s41597-020-0453-3

Hawkins, E., & Sutton, R. (2011). The potential to narrow uncertainty in projections of regional precipitation change. *Climate Dynamics*, *37*, 407–418. https://doi.org/10.1007/s00382-010-0810-6

Hurrell, J. W., Holland, M. M., Gent, P. R., Ghan, S., Kay, J. E., Kushner, P. J., & Marshall, S. (2013). The Community Earth System Model: A framework for collaborative research. *Bulletin of the American Meteorological Society*, *94*(9), 1339–1360. https://doi.org/10.1175/BAMS-D-12-00121.1

Kay, J. E., Deser, C., Phillips, A., Mai, A., Hannay, C., Strand, G., & Vertenstein, M. (2015). The Community Earth System Model (CESM) Large Ensemble Project: A community resource for studying climate change in the presence of internal climate variability. *Bulletin of the American Meteorological Society*, *96*(8), 1333–1349. https://doi.org/10.1175/BAMS-D-13-00255.1

Kirtman, B. P., Min, D., Infanti, J. M., Kinter, J. L., Paolino, D. A., Zhang, Q., & Wood, E. F. (2014). The North American Multimodel Ensemble: Phase-1 Seasonal-to-Interannual Prediction; Phase-2 toward developing Intraseasonal Prediction. *Bulletin of the American Meteorological Society*, *95*(4), 585–601. https://doi.org/10.1175/BAMS-D-12-00050.1

Lader, R., Walsh, J. E., Bhatt, U. S., & Bieniek, P. A. (2017). Projections of twenty-first-century climate extremes for Alaska via dynamical downscaling and quantile mapping. *Journal of Applied Meteorology and Climatology*, *56*(9), 2393–2409. https://doi.org/10.1175/JAMC-D-16-0415.1

Loranty, M. M., Berner, L. T., Goetz, S. J., Jin, Y., & Randerson, J. T. (2014). Vegetation controls on northern high latitude snow-albedo feedback: Observations and CMIP5 model simulations. *Global Change Biology*, *20*(2), 594–606. https://doi.org/10.1111/gcb.12391

Maher, N., Milinski, S., Suarez-Gutierrez, L., Botzet, M., Dobrynin, M., Kornblueh, L., & Marotzke, J. (2019). The Max Planck Institute Grand Ensemble: Enabling the exploration of climate system variability. *Journal of Advances in Modeling Earth Systems*, *11*(7), 2050–2069. https://doi.org/10.1029/2019MS001639

Mearns, L. O., McGinnis, S., Korytina, D., Arritt, R., Biner, S., Bukovsky, M., et al. (2017). *The NA-CORDEX dataset version 1.0*. https://doi.org/10.5065/D6SJ1JCH

Melvin, A. M., Larsen, P., Boehlert, B., Neumann, J. E., Chinowsky, P., Espinet, X., et al. (2017). Climate change damages to Alaska public infrastructure and the economics of proactive adaptation. *Proceedings of the National Academy of Sciences*, *114*(2), E122–E131. https://doi.org/10.1073/pnas.1611056113

Monier, E., & Gao, X. (2014). Climate change impacts on extreme events in the United States: An uncertainty analysis. *Climatic Change*, *131*, 67–81. https://doi.org/10.1007/s10584-013-1048-1

Morice, C. P., Kennedy, J. J., Rayner, N. A., & Jones, P. D. (2012). Quantifying uncertainties in global and regional temperature change using an ensemble of observational estimates: The HadCRUT4 dataset. *Journal of Geophysical Research*, *117*, D08101. https://doi.org/10.1029/2011JD017187

O'Neill, B. C., Tebaldi, C., van Vuuren, D. P., Eyring, V., Friedlingstein, P., Hurtt, G., et al. (2016). The Scenario Model Intercomparison Project (ScenarioMIP) for CMIP6. *Geoscientific Model Development*, *9*(9), 3461–3482. https://doi.org/10.5194/gmd-9-3461-2016

Overland, J. E., Hanna, E., Hanssen-Bauer, I., Kim, S.-J., Walsh, J. E., Wang, M., et al. (2020). *Surface air temperature*. Retrieved from https://www.arctic.noaa.gov/Report-Card/Report-Card-2019/ArtMID/7916/ArticleID/835/Surface-Air-Temperature

Overland, J. E., & Wang, M. (2021). The 2020 Siberian heat wave. *International Journal of Climatology*, *41*(S1), E2341–E2346. https://doi.org/10.1002/joc.6850

Partain, J. L., Alden, S., Bhatt, U. S., Bieniek, P. A., Brettschneider, B. R., Lader, R. T., & Ziel, R. H. (2016). An assessment of the role of anthropogenic climate change in the Alaska fire season of 2015. *Bulletin of the American Meteorological Society*, *97*(12), S14–S18. https://doi.org/10.1175/bams-d-16-0149.1

Rohde, R., Muller, R., Jacobsen, R., Perlmutter, S., Rosenfeld, A., Wurtele, J., et al. (2013). A new estimate of the average Earth surface land temperature spanning 1753 to 2011. *Geoinformatics Geostatistics: An Overview*, *1*. https://doi.org/10.4172/2327-4581.1000101

Rohde, R., Muller, R. A., Jacobsen, R., Muller, E., Perlmutter, S., Rosenfeld, A., et al. (2013). Berkeley Earth temperature averaging process. *Geoinformatics Geostatistics: An Overview*, *1*. https://doi.org/10.4172/gigs.1000103

Sherwood, S. C., Webb, M. J., Annan, J. D., Armour, K. C., Forster, P. M., Hargreaves, J. C., et al. (2020). An assessment of Earth's climate sensitivity using multiple lines of evidence. *Reviews of Geophysics*, *58*(4), e2019RG000678. https://doi.org/10.1029/2019RG000678

Steele, M., Ermold, W., & Zhang, J. (2008). Arctic Ocean surface warming trends over the past 100 years. *Geophysical Research Letters*, *35*(2), L02614. https://doi.org/10.1029/2007GL031651

Strader, H., & Stevens, E. (2019). *2019 fire season weather summary*. Retrieved from https://fire.ak.blm.gov/content/Weather%20Folder/Fire%20Season%20Summaries/2019%20Fire%20Season.pdf

Thoman, R., & Brettschneider, B. (2016). Hot Alaska: As the climate warms, Alaska experiences record high temperatures. *Weatherwise*, *69*(6), 12–20. https://doi.org/10.1080/00431672.2016.1226639

Thorsteinson, L., & Love, M. (Eds.). (2016). *Alaska Arctic Marine Fish Ecology Catalog* (Vol. 76). https://doi.org/10.3133/sir20165038

Voiland, A., Daughin, L., & Young, A. (2019). *Historic heat in Alaska*. Retrieved from https://earthobservatory.nasa.gov/images/145294/historic-heat-in-alaska

Walsh, J. E., Thoman, R. L., Bhatt, U. S., Bieniek, P. A., Brettschneider, B., Brubaker, M., & Partain, J. (2018). The high latitude marine heat wave of 2016 and its impacts on Alaska. *Bulletin of the American Meteorological Society*, *99*(1), S39–S43. https://doi.org/10.1175/BAMS-D-17-0105.1

Willmott, C. J., & Matsuura, K. (2001). *Terrestrial air temperature and precipitation: Monthly and annual time series (1950–1999)*. Retrieved from http://climate.geog.udel.edu/?climate/html_pages/README.ghcn_ts2.html

Young, A. M., Higuera, P. E., Duffy, P. A., & Hu, F. S. (2017). Climatic thresholds shape northern high-latitude fire regimes and imply vulnerability to future climate change. *Ecography*, *40*(5), 606–617. https://doi.org/10.1111/ecog.02205

Yu, Y., Dunne, J. P., Shevliakova, E., Ginoux, P., Malyshev, S., John, J. G., & Krasting, J. P. (2021). Increased risk of the 2019 Alaskan July fires due to anthropogenic activity. *Bulletin of the American Meteorological Society*, *102*(1), S1–S7. https://doi.org/10.1175/BAMS-D-20-0154.1